

Preparation of T-2 toxin-containing pH-sensitive liposome and its antitumor activity

YUAN DONG¹, GUIXIAN MENG¹, JIAN GUO¹, MOLI YIN², HUIJING XU¹, YUJIE LI¹,
JIE ZHU^{1,3}, WENHE ZHU², MINGGUANG LI¹, YAN LI¹ and HUIYAN WANG²

¹Department of Laboratory Medicine, Jilin Medical University;

²Jilin Collaborative Innovation Center for Antibody Engineering, Jilin Medical University, Jilin 132013;

³College of Life Science, Jilin University, Changchun, Jilin 130510, P.R. China

Received February 23, 2020; Accepted August 14, 2020

DOI: 10.3892/mmr.2020.11531

Abstract. T-2 toxin is a type A trichothecene mycotoxin. In order to reduce the side effects of T-2 toxin and increase the tumor targeting ability, a pH-sensitive liposome of T-2 toxin (LP-pHS-T2) was prepared and characterized in the present study. The cytotoxicity of LP-pHS-T2 on A549, Hep-G2, MKN-45, K562 and L929 cell lines was tested by 3-(4,5-dimethylthiazolyl-2)-2,5-diphenyltetrazolium bromide assay, with T-2 toxin as the control. The apoptotic and migratory effects of LP-pHS-T2 on Hep-G2 cells were investigated. The preparation process of LP-pHS-T2 involved the following parameters: Dipalmitoyl phosphatidylcholine: dioleoylphosphatidylethanolamine, 1:2; total phospholipid concentration, 20 mg/ml; phospholipid:cholesterol, 3:1; 4-(2-hydroxyethyl)-1-piperazineethanesulfonic acid buffer (pH 7.4), 10 ml; drug:lipid ratio, 2:1; followed by ultrasound for 10 min and extrusion. The encapsulation efficiency reached 95±2.43%. The average particle size of LP-pHS-T2 after extrusion was 100 nm; transmission electron microscopy showed that the shape of LP-pHS-T2 was round or oval and of uniform size. The release profile demonstrated a two-phase downward trend, with fast leakage of T-2 toxin in the first 6 h (~20% released), followed by sustained release up to 48 h (~46% released). From 48-72 h, the leakage rate increased (~76% released), until reaching a minimum at 72 h. When LP-pHS-T2 was immersed in 0.2 mol/l disodium phosphate-sodium dihydrogen phosphate buffers (pH 6.5), the release speed was significantly increased and the release rate reached 91.2%, demonstrating strong pH sensitivity. Overall, antitumor tests showed that LP-pHS-T2 could promote the apoptosis and inhibit the migration of Hep-G2 cells. The present study provided a new approach for the development of T-2 toxin-based anti-cancer drugs.

Introduction

T-2 toxin (4β,15-diacetoxy-8α-(3-methylbutyryloxy)-3α-hydroxy-12, 13-epoxytrichothecene-9-ene; C₂₄H₃₄O₉) (relative molecular weight 466.52), a type A trichothecene mycotoxin, is the secondary metabolite of *Fusarium sporotrichioides* and *F. Langsethiae* (1,2). T-2 toxin is found extensively in moldy cereals (wheat, maize, barley and oats) and moldy food (3). It is acknowledged as an unavoidable contaminant in human foods (4). Exposure to T-2 toxin causes oral injury (5), liver injury (6), decrease in body weight, gastrointestinal injury and even mortality (7). The severe tissue damage caused by T-2 toxin is associated with the inhibition of protein and DNA synthesis, metabolic alteration, cell membrane injury, immunosuppression, and glycoprotein and collagen synthesis (8-10), thus resulting in apoptosis. T-2 toxin poses great harm to the health of human beings and livestock.

Early studies on T-2 toxin only focused on toxicology and metabolism aspects (11-13). In the 20th century, it was reported that T-2 toxin has toxic effects on a number of cancer cell types (14). T-2 toxin can induce apoptosis in HL-60 promyelocytic leukemia cells and hepatocellular carcinoma cells (15). The mechanism of apoptosis induced by T-2 toxin is proposed to be linked with oxidative stress and the activation of caspase 3/9 and the mitochondrial pathway (16,17). Therefore, the toxin possesses potential applications in tumor treatment. However, due to the toxicity of T-2 toxin on normal cells, T-2 by itself does not exhibit selectivity for tumoral tissues and hence might be characterized by a low therapeutic index. A search for an alternative strategy is required.

The use of targeted drugs is a valuable method to solve the aforementioned selectivity issues (18). Liposomes are phospholipid bilayer vesicles that possess great potential for application in the targeted delivery of chemotherapeutics in the treatment of cancer (19). The use of liposomes as drug carriers for chemotherapeutic targeting to tumor tissues is based on their greater advantages compared with other dosage methods, due to their low systemic toxicity, bioavailability and the capability to enhance the solubility of a range of chemotherapeutic agents, in addition to their ability for encapsulation of hydrophilic and lipophilic drugs (20). Liposomes can reduce drug toxicity without changing drug efficacy against tumor cells,

Correspondence to: Professor Huiyan Wang, Jilin Collaborative Innovation Center for Antibody Engineering, Jilin Medical University, 5 Jilin Avenue, Jilin 132013, P.R. China
E-mail: zswwhy518@163.com

Key words: T-2 toxin, pH sensitivity, liposomes, antitumor activity

making them a highly efficient targeting drug carrier (21). Liposomes enhance the anticancer drug therapeutic index by increasing the drug concentration in tumor cells through tumor targeting (22). The most advanced targeting strategies proposed for treating cancer involve the development of multifunctional liposomes, with combined targeting mechanisms. There are a number of types of targeting strategies for liposomes, such as temperature-, light-, redox reagent- and pH-sensitive (23-25). Due to their characteristics of targeting the acidic tumor microenvironment (pH 6.8-6.5), pH-sensitive liposomes have received much attention recently (26,27). pH-sensitive liposomes consist of phosphatidylcholine or dioleoylphosphatidylethanolamine (DOPE), which are stable at physiological pH (pH 7.4), but undergo destabilization under acidic conditions (28). Various antitumor drug-containing pH-sensitive liposomes have been successfully prepared, such as those for 5-fluorouracil, doxorubicin (DOX) and taxol (29-31).

The objective of the present study was to design and optimize the preparation process of a novel pH-sensitive liposomal delivery system containing T-2 toxin (LP-pHS-T2). The particle size, stability and pH-sensitivity of the liposomes in buffers were determined. Furthermore, the antitumor activity of pHS-LP-T2 was evaluated *in vitro*. This is an exploration of T-2 toxin as a new antitumor drug.

Materials and methods

Reagents. 1,2-Dioleoyl-3-trimethylammonium-propane (DOTAP), 1,2-distearoyl-sn-glycero-3-phosphoethanolamine-N-[methoxy(polyethylene glycol)-2000] (DSPE-mPEG-2000), 1,2-dioleoyl-sn-glycero-3-phosphocholine (DOPC), dipalmitoyl phosphatidylcholine (DPPC), DOPE and cholesterol (chol) were purchased from Shanghai Dongshang Biotechnology Co., Ltd. 3-(4,5-Dimethylthiazolyl-2)-2,5-diphenyltetrazolium bromide (MTT), Hoechst 33342, propidium iodide (PI), NaCl, HCl, high performance liquid chromatography (HPLC) grade methanol and 4-(2-hydroxyethyl)-1-piperazineethanesulfonic acid (HEPES) sodium salt were purchased from Thermo Fisher Scientific, Inc. Dulbecco's modified Eagle's medium (DMEM) and fetal bovine serum (FBS) were purchased from Gibco; Thermo Fisher Scientific, Inc.

T-2 toxin was separated and purified from corn contaminated with *Fusarium sporotrichioides* by graduated organic solvent extraction, silica column chromatography and preparative HPLC, as previously described (32). Purity, >98%, the three-dimensional HPLC chromatogram of T-2 toxin is shown in Fig. S1.

The A549, Hep-G2, MKN-45 and K562 cell lines are human tumor cell lines and were kept at -80°C; L929 cells are mouse fibroblast cells (normal cells) and were kept at -80°C. All cell lines were purchased from the American Type Culture Collection. All cells were incubated in DMEM with 10% FBS and 1% antibiotics in a humidified atmosphere containing 5% CO₂/95% air at 37°C. The Hep-G2 cells were authenticated as a hepatoma cell line using short tandem repeats (STR) profiling.

HPLC analysis of T-2 toxin. The concentration of T-2 toxin was determined using a HPLC system (Waters Corporation) equipped with an Agilent ZORBAX SB-C3 column (250x4.6 mm, 5 μm; Agilent Technologies Inc.). The mobile phase was methanol/water (60:40, v/v) driven by a double pump

(Waters 150; Waters Corporation) at a flow rate of 1 ml/min. The amount of T-2 toxin was detected at absorption wavelengths of 198 nm with an injection volume of 10 μl at 30°C. Each sample was spiked with 6 ng/ml T-2 toxin as the internal standard. Each run was performed in triplicate. T-2 toxin limit of detection was determined by dissolving T-2 toxin at decreasing concentrations in methanol until the signal-to-noise ratio was equal to 3. According to the previous methods (33), the linearity of the standard curves, intraday and interday precision, and accuracy were determined using six T-2 toxin concentrations of 100, 200, 400, 600, 800 and 1,000 μg/ml.

Preparation of liposomes. Due to the hydrophobicity of T-2 toxin and its high solubility in methanol, T-2 toxin was wrapped in the lipid bilayer of the liposome. T-2 toxin-loaded pH-sensitive liposomes were prepared using the thin-film hydration method (34). In brief, T-2 toxin or DPPC:DOPE:chol at 1:2:1 (weight:weight:weight) was dissolved in ethanol, respectively. T-2 toxin and phospholipid mixture were mixed in a ratio of 1:1, 1:2, 1:3, 2:1, 4:1, 5:1, 6:1 or 10:1 and a total phospholipid concentration of 5, 10, 15, 20 or 25 mg/ml, respectively. The ethanol was then removed using a rotary evaporator at 40°C, until a uniform film was formed at the bottom of the flask. The film was hydrated with an appropriate volume of 20 mM HEPES buffer solution for 1 h. Liposomes were sonicated with a 20-kHz frequency probe-type sonicator (Xinhi Biolab Co., Ltd.) at 300 W for 10 min with 5-sec intervals in an ice bath. After ultrasonication, titanium particles released from the probe were removed by centrifugation at 2,000 x g for 10 min at room temperature. Free T-2 toxin was removed by ultrafiltration with a 300 K membrane filter (pore size 0.2 μm; Sartorius Stedim Biotech; Sartorius AG) at 6,000 x g for 30 min at room temperature. Finally, the liposomes were filtered through a NanoAble-150 Extruder (PhD Technology LLC) equipped with a 200-μm pores of polycarbonate membrane three times. An equal volume of 60% methanol was added to the liposomes to release T-2 toxin from the inside of the liposomes. The amount of released T-2 toxin in the liposomes was determined by HPLC and the entrapment efficiency of LP-pHS-T2 was calculated according to the following equation: EE (%) = $W_{\text{encapsulated}}/W_{\text{total}} \times 100$, where EE is entrapment efficiency, W_{total} is the total amount of T-2 toxin initially added in the liposome preparation and $W_{\text{encapsulated}}$ is the amount of T-2 toxin encapsulated into the liposomes.

Liposome characterization

Particle size and ζ potential. The particle diameter, polydispersity index (PDI) value and ζ potential of LP-pHS-T2 were measured by laser light scattering using a particle size analyzer according to the manufacturer's protocol (Zetasizer 3000HSA; Malvern Instruments, Ltd.) (35). The determination was repeated three times for each sample.

Morphology. The morphology of the LP-pHS-T2 was observed using a transmission electron microscope (TEM; FEI; Thermo Fisher Scientific, Inc.). For TEM studies, the LP-pHS-T2 was two-fold diluted with deionized water, and the final dilution of 0.25 mg/ml was placed on the surface of a copper grid. Next, 2% aqueous solution of sodium phosphotungstate was added for negative staining at room temperature for 15 min. Following

air-drying, the copper grid was placed in the TEM (magnification, x2,000) and imaged using Gatan DigitalMicrograph software version 1.4.3 (Gatan, Inc.) (35).

Drug release profile in vitro. The release of T-2 toxin from LP-pHS-T2 *in vitro* was monitored using a dialysis method (35). LP-pHS-T2 (1 ml) was added into a dialysis bag with a molecular weight cutoff of 6,000-8,000 Da and immersed in 20 ml phosphate-buffered solution (pH 7.4) at 37°C for 0, 1, 2, 4, 8, 12, 24, 48 or 72 h. An equal volume of 60% methanol was added to the liposomes. The amount of T-2 toxin released at each time point was determined by HPLC.

Stability of LP-pHS-T2 at different pH values. LP-pHS-T2 (1 ml) was added into a 6,000 to 8,000-Da molecular weight-cutoff dialysis bag and immersed in 1/15 mol/l disodium hydrogen phosphate-potassium dihydrogen phosphate buffer (pH 5) or a series of 0.2 mol/l disodium phosphate-sodium dihydrogen phosphate buffers (pH 5, 5.5, 6, 6.5 and 7) at 37°C for 30 min. An equal volume of 60% methanol was added to the liposomes. The amount of T-2 toxin released was determined by HPLC as aforementioned.

Antitumor activity of LP-pHS-T2

Cytotoxicity assay. MTT assay was used to evaluate the cytotoxicity of T-2 or LP-pHS-T2 on A549, Hep-G2, MKN-45, K562 and L929 cell lines (36). The cells were seeded on 96-well culture plates at a density of 5×10^5 cells/well. Following incubation overnight, fresh medium containing T-2 toxin or LP-pHS-T2 at final concentrations of 0.5, 5, 10 and 15 $\mu\text{g/ml}$ was added to the cells at 37°C. After incubation for 48 h at 37°C, the plates were washed with PBS and incubated with 5 mg/ml MTT for 4 h at 37°C in darkness. The supernatant was aspirated and 100 μl DMSO was added to each well to dissolve the purple formazan crystals. After continuous agitation for 15 min, the reaction product was quantified by measuring the absorbance at 495 nm using a Multi-plate Reader (Model 680; Bio-Rad Laboratories Inc.). The IC_{50} values for each cell line were calculated using the GraphPad prism 7.0 software (GraphPad Software, Inc.) and compared between T-2 toxin and LP-pHS-T2.

Apoptosis detection using Hoechst staining. Hep-G2 cells were randomly selected from the four tumor cell lines and cultured in six-well plates for 24 h at 37°C, with a density of 5×10^5 cells/well. The cells were treated with 10 $\mu\text{g/ml}$ of T-2 or LP-pHS-T2 at 37°C. After 4 h of incubation, the cells were fixed with 4% paraformaldehyde at 37°C, followed by staining with Hoechst 33342 to stain the nucleus for 30 min at 37°C in darkness (36). Cell imaging was performed with a fluorescence inverted microscope combined with cellSens standard version 1.5 software (magnification, x20; IX70; Olympus Corporation). Areas of cells stained with blue fluorescence were imaged. Each group was imaged three times and the picture with the most stained cells was selected.

Migration assay. The Hep-G2 cells were plated in 6-well plates, cultured to 100% confluence at 37°C for 24 h, and then scratched with a p200 pipette tip (diameter, 0.57 mm). The plates were washed with PBS three times. Fresh serum-free medium containing 10 $\mu\text{g/ml}$ T-2 toxin or LP-pHS-T2

Table I. Establishment of T-2 toxin detection.

Detection parameter	Value
RSD, %	
Intraday precision	1.42±0.14
Interday precision	1.94±0.58
Accuracy	2.93±0.15
Limit of detection, $\mu\text{g/ml}$	14.78±0.85

was added to the cells. After 24-h culture, the distances of migrating cells were analyzed to evaluate the cell migratory ability by a fluorescence inverted microscope combined with cellSens standard version 1.5 software (magnification, x20; IX70; Olympus Corporation), which was performed as previously described (37). The average width of the wound was measured.

Apoptosis detection via flow cytometry. The Hep-G2 cells (5×10^5 cells/sample) were incubated in 6-well plates at 37°C. T-2 or LP-pHS-T2 (10 $\mu\text{g/ml}$) was added to the cells, which were incubated at 37°C for 18 h. Apoptosis was measured by a PI/Annexin V-FITC dual-staining kit (Thermo Fisher Scientific, Inc.), according to the manufacturer's protocols, and a BD Accuri™ C6 flow cytometer (BD Biosciences) combined with cFlow version 1.023.1 software, as previously described (38). Each assay was repeated in triplicate.

Statistical analysis. All data were analyzed by Origin 8.0 (OriginLab Corporation) and are presented as the mean \pm standard deviation. All data were measured in triplicate. The results were in normal distribution. The statistical significance among multiple groups was evaluated using one-way ANOVA followed by Tukey's post hoc test. $P < 0.05$ was considered to indicate a statistically significant difference.

Results

T-2 toxin detection using HPLC. HPLC was used to determine the concentration of T-2 toxin. The standard curve, the intraday precision, the interday precision, the accuracy and the limit of detection were investigated (Table I); the linear regression equation was $y = 11393.41x + 14937.51$ (where x = concentration of T-2 toxin in $\mu\text{g/ml}$ and y = the peak area) and the coefficient of determination was $R^2 = 0.999$, indicating good linearity. Intraday ($n=3$) and interday ($n=3$) precision was not $>10\%$ in any of the assays. The limit of detection was $14.78 \pm 0.85 \mu\text{g/ml}$.

Preparation and characterization of liposomes

Optimization of liposome preparation process by a single factor experiment. On the basis of preliminary experiments, the effects of six influencing factors [type of phospholipid, DPPC:DOPE (w/w), phospholipids:chol (w/w), hydration volume, phospholipid concentration and drug-lipid ratio] on EE values were investigated by a single factor experiment. As presented in Fig. 1A, several phospholipids commonly used in the preparation of pH-sensitive liposomes, including DOTAP, DOPE, DPPC, DSPE-mPEG-2000 and DOPC, were investigated. DOPE and

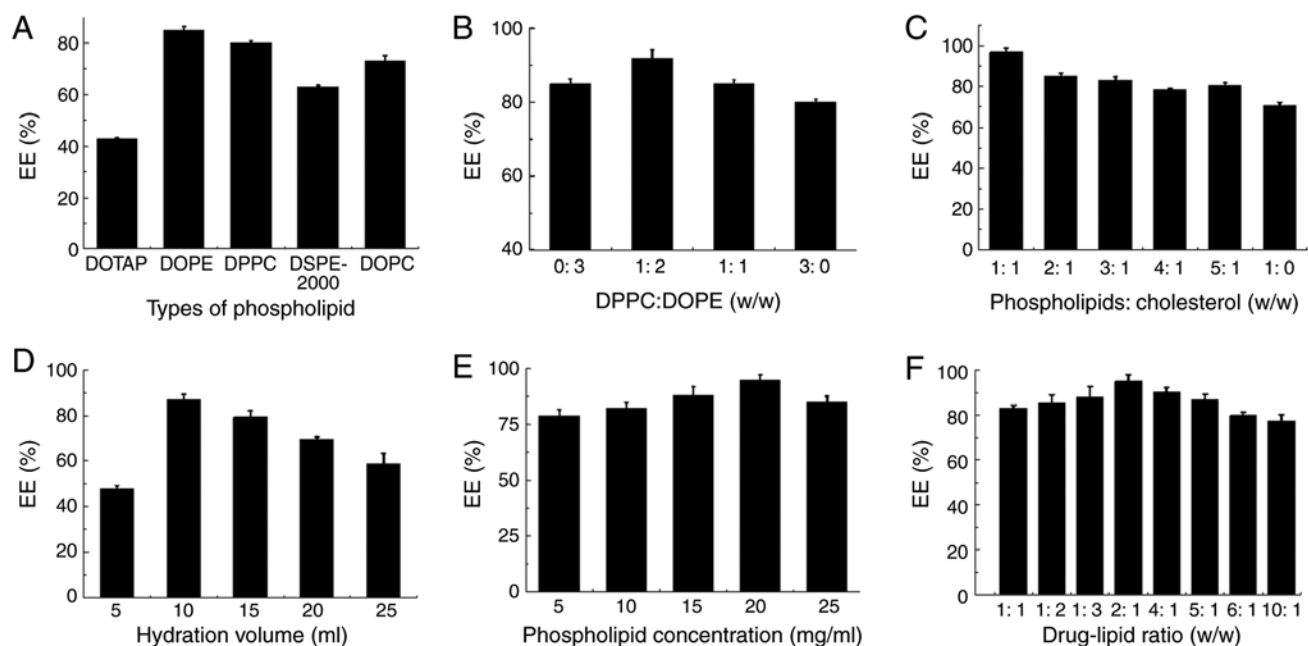


Figure 1. Factors that influence the EE values of liposomes. Effects of (A) types of phospholipid, (B) DPPC:DOPE (w/w), (C) phospholipids:cholesterol (w/w), (D) hydration volume, (E) phospholipid concentration and (F) drug-lipid ratio on EE investigated by a single factor experiment. Data are expressed as mean \pm standard deviation ($n=3$). DOTAP, 1,2-dioleoyl-3-trimethylammonium-propane; DOPE, dioleoylphosphatidylethanolamine; DPPC, dipalmitoyl phosphatidylcholine; DSPE-mPEG-2000, 1,2-distearoyl-sn-glycero-3-phosphoethanolamine-N-[methoxy(polyethylene glycol)-2000]; DOPC, 1,2-dioleoyl-sn-glycero-3-phosphocholine; EE, entrapment efficiency.

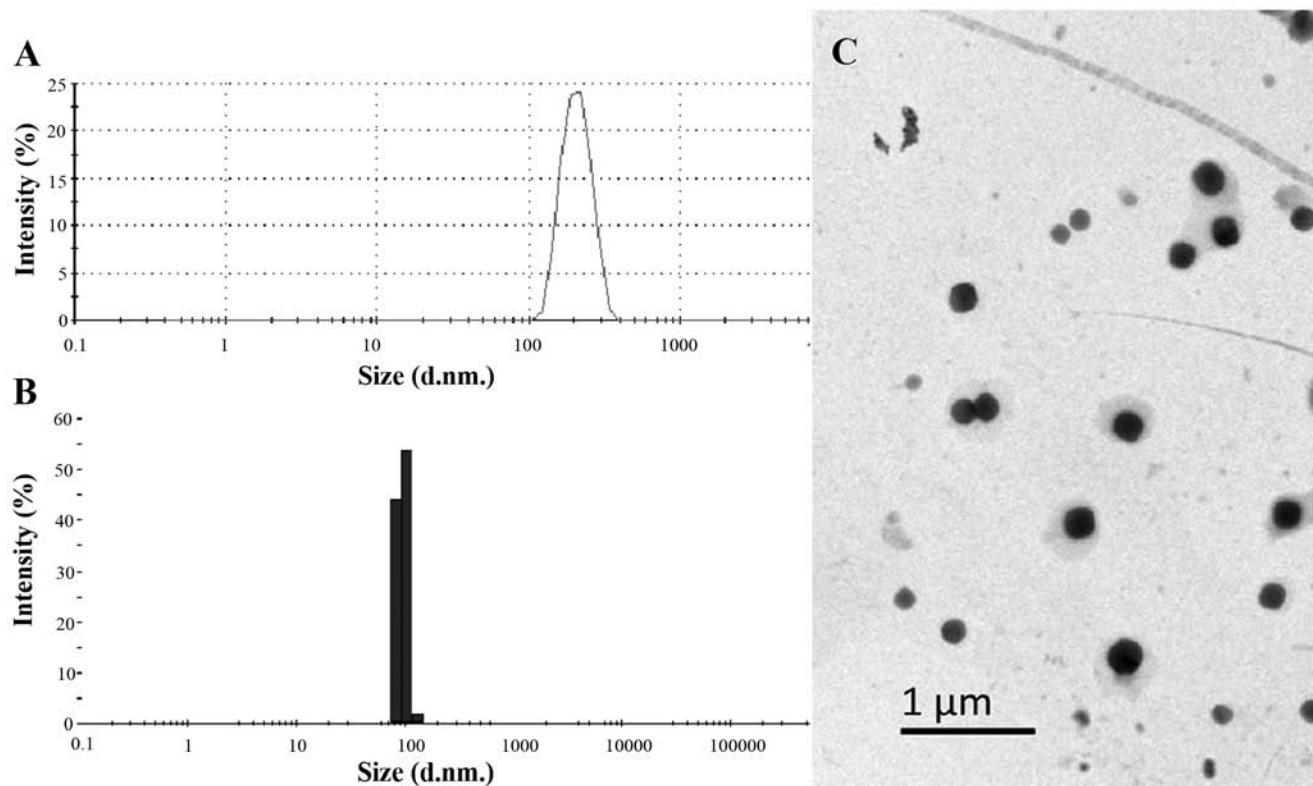


Figure 2. Particle size and morphology of liposomes. Mean particle size of LP-pHS-T2 (A) before and (B) after extrusion, as measured by a particle size analyzer, where d.nm represents the mean particle size of the particle. (C) Transmission electron microscope image of LP-pHS-T2 (magnification, x2,000). LP-pHS-T2, liposomal delivery system containing T-2 toxin.

DPPC were the most efficient phospholipids for encapsulating T-2 toxins, hence were chosen for the following experiments. Similarly, the highest EE values was obtained when the T-2

toxin or DPPC:DOPE:chol=1:2:1 (w/w/w) were mixed at the total phospholipid concentration of 20 mg/ml and drug-lipid ratio of 2:1 (w/w) and hydrated with 10 ml of 20 mM HEPES

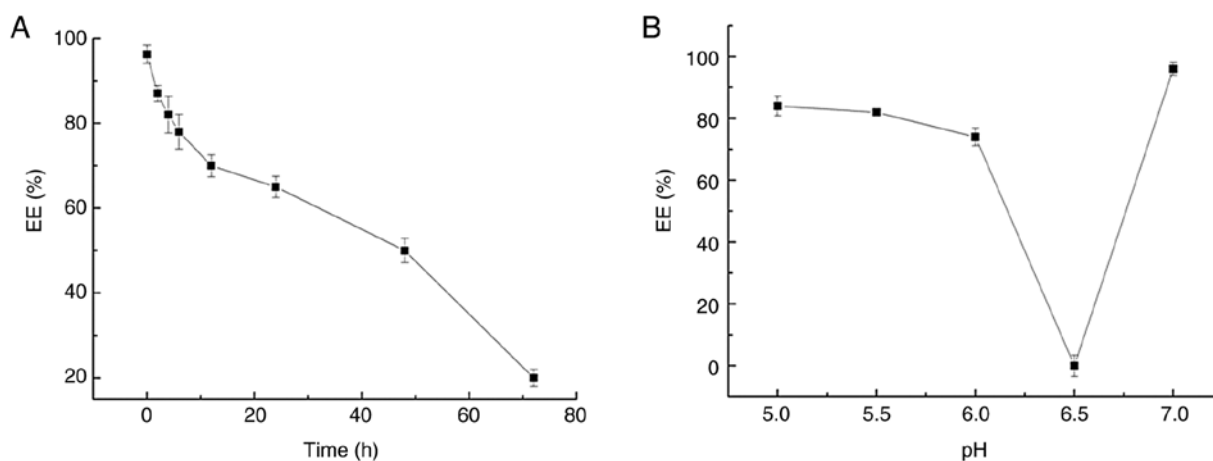


Figure 3. Drug release profile and pH sensitivity of liposomes. EE values of LP-pHS-T2 at (A) each time point and (B) different pH values. Data are expressed as mean \pm standard deviation (n=3). EE, entrapment efficiency; LP-pHS-T2, liposomal delivery system containing T-2 toxin.

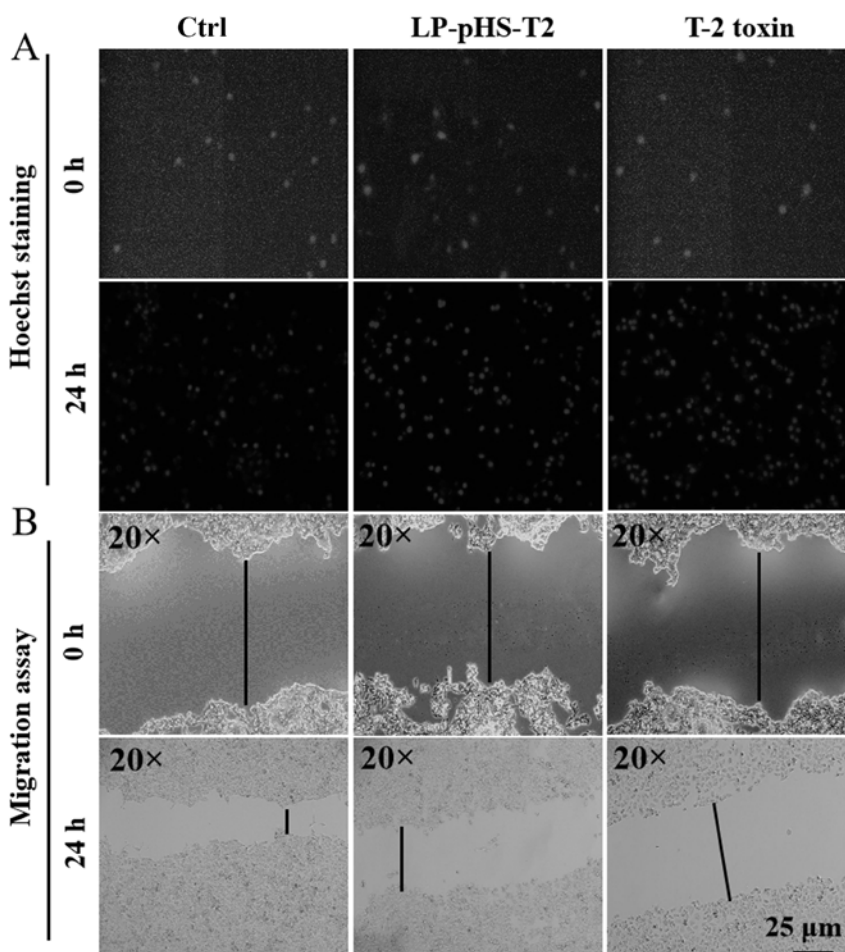


Figure 4. Antitumor activity of LP-pHS-T2 and T-2 toxin detected by Hoechst staining and wound healing assay. (A) LP-pHS-T2 and T-2 toxin induced apoptosis (nuclear morphology) of Hep-G2 cells, as examined by Hoechst 33342 staining (magnification, x20). (B) LP-pHS-T2 and T-2 toxin treatment inhibited the migration ability of Hep-G2 cells, as determined by wound healing assay (magnification, x20). LP-pHS-T2, liposomal delivery system containing T-2 toxin; CTRL, control.

buffer solution as shown in Fig. 1B-F. Next, after sonication and extrusion, the maximum EE was $95 \pm 2.43\%$.

Characterization of LP-pHS-T2. The mean particle size of LP-pHS-T2 was ~ 267 nm before extrusion (Fig. 2A) and

100 nm after extrusion (Fig. 2B). These nanoparticles ranging from 100-150 nm possess advantages in controllable pore diameter and biocompatibility (39). Data from the particle size analyzer showed that the ζ potential was -29.3 mV, which demonstrated that LP-pHS-T2 was stable at room

Table II. IC₅₀ values of T-2 toxin and LP-pHS-T2 by 3-(4,5-dimethylthiazolyl-2)-2,5-diphenyltetrazolium bromide assay at pH 7.4.

Cell line	T-2 toxin, ng/ml	LP-pHS-T2, ng/ml
A549	150.68±0.85	174.38±2.46
HepG-2	210.41±8.14	253.41±5.47
MKN-45	213.13±6.48	249.36±9.61
K562	11.59±1.05	43.42±2.87 ^a
L929	1437.53±20.80	1864.24±20.47 ^b

^aP<0.01 and ^bP<0.05 vs. T-2 toxin group. LP-pHS-T2, liposomal delivery system containing T-2 toxin.

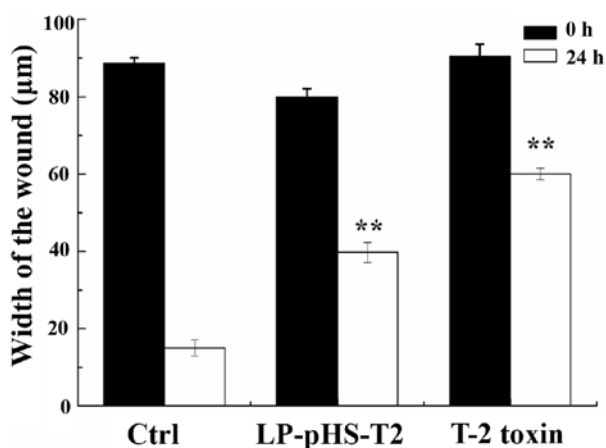


Figure 5. Average wound width in each group of the wound healing assay. Data are expressed as the mean ± standard deviation (n=3). **P<0.01 vs. CTRL. LP-pHS-T2, liposomal delivery system containing T-2 toxin; CTRL, control.

temperature (40). The PDI value was 0.216, which indicated a moderate dispersion of nanoparticles (data not shown). The morphology of LP-pHS-T2 was found to be homogeneous and spherical when visualized under a TEM (Fig. 2C).

Release profile of LP-pHS-T2 at different time points and pH values. The release profile of T-2 toxin from LP-pHS-T2 *in vitro* was monitored within 72 h at 37°C (pH 7.4). The results are shown in Fig. 3A. The release profile demonstrated a two-phase downward trend, with fast leakage of T-2 toxin in the first 6 h (~20% released), followed by sustained release up to 48 h (~46% released). From 48 to 72 h, the leakage rate increased (~76% released), until reaching a minimum at 72 h. The stability of LP-pHS-T2 at different pH values is shown in Fig. 3B. The release amount of T-2 toxin was up to 91.2% when the pH was 6.5, which indicated that LP-pHS-T2 may be structurally unstable under this faintly acid condition and release T-2 toxin.

Antitumor activity of LP-pHS-T2

LP-pHS-T2 possesses cytotoxicity effects on tumor cells. MTT assay was employed to test the inhibition rate of T-2 toxin and LP-pHS-T2 on a series of tumor cells and a normal cell line, L929. The IC₅₀ values of each group are shown in Table II.

T-2 toxin and LP-pHS-T2 exhibited good antitumor activity at the same concentration (P>0.05), which indicated that the proposed liposomal formulation did not noticeably reduce the therapeutic index and that T-2 toxin could be released gradually. However, possibly due to the sustained release of liposomes, only the IC₅₀ values of LP-pHS-T2 on K562 cells were slightly higher compared with T-2 toxin alone. In addition, the IC₅₀ value of LP-pHS-T2 in normal cells (L929 cells) was significantly higher compared with that of T-2 toxin (P<0.05), which demonstrated the reduction of T-2 side effects as result of its encapsulation.

Apoptosis analysis using Hoechst staining. The nucleus of apoptotic cells can be stained dense blue using Hoechst 33342. The results from the present study are shown in Fig. 4A and they demonstrate that T-2 toxin and LP-pHS-T2 at dose of 10 µg/ml markedly induced apoptosis in Hep-G2 cells, as indicated by the enhanced intensity of blue fluorescence.

Wound healing assay. Certain tumor cells are capable of migration. Thus, a wound-healing assay was performed to observe the inhibitory effect of T-2 toxin and LP-pHS-T2 on the migration ability in Hep-G2 cells. The results are shown in Fig. 4B. After a 24-h incubation, the wound areas in the control group were almost healed. By contrast, the migration ability in the Hep-G2 cells was significantly inhibited after T-2 toxin or LP-pHS-T2 treatment at 10 µg/ml as shown in Fig. 5 (P<0.05).

Apoptosis detection via flow cytometry. The nucleic acid dye PI and Annexin V can differentiate early apoptosis from late apoptosis and necrotic cells. As shown in Fig. 6, the percentage of total apoptotic cells increased nearly two-fold after T-2 toxin or LP-pHS-T2 treatment in Hep-G2 cells compared with that in the control group (P<0.05).

Discussion

It is known that T-2 toxin has strong toxicity (41,42) and thus a great advantage in killing cancer cells. However, due to the toxic side effects on normal cells, the use of T-2 toxin in the clinic is limited. Studies on targeted agents appear to be the only solution. Attempts have been made to prepare T-2 toxin-conjugated antibody drugs, but no substantial progress has occurred (43).

As a novel type of nano drug carrier, pH-sensitive liposomes have been widely studied in tumor therapy for their advantages of tumor-targeting and sustained release (44). Changes in pH in the tumor microenvironment can cleave the linkages between liposomes and drugs, and prompt drug release to the specific tumor tissues (45). In a previous study, DOX loaded into pH-sensitive micelles exhibited an enhanced cytotoxic effect in MCF-7 cancer cells (46). Dextran sulfate-DOX and alginate-cisplatin polymer-drug complex-loaded liposomes also exhibit specific receptor-mediated endocytic uptake in cancer cells (47). In the present study, a pH-sensitive liposome containing T-2 toxin was prepared. In the preparation process, the EE value was affected mainly by the type of biomaterials, the loading method, the hydration volume and the drug-lipid ratio. The density of T-2 toxin is twice that of phospholipids. As a fat-soluble small molecule drug, T-2 toxin is mainly

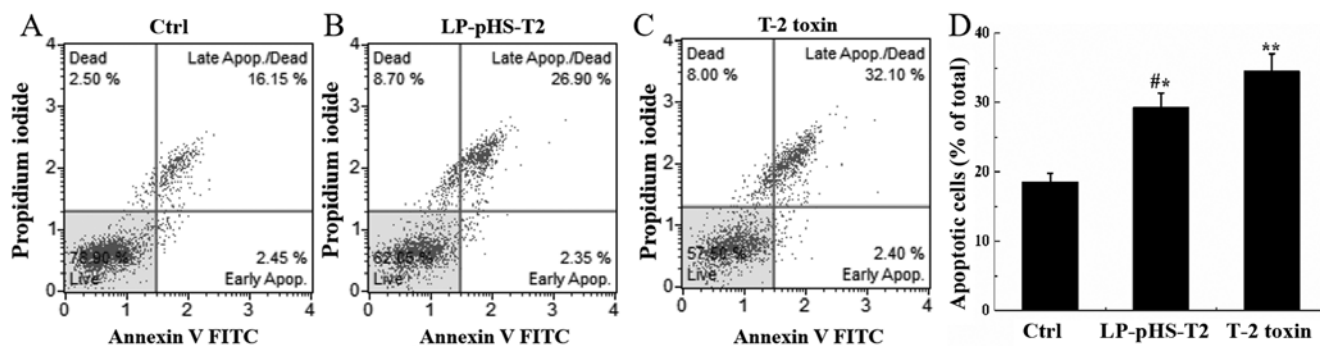


Figure 6. Apoptosis detection via flow cytometry. Apoptotic rates in (A) CTRL and caused by (B) LP-pHS-T2 and (C) T-2 (C) toxin measured by a PI/Annexin V-FITC dual-staining kit using flow cytometry. (D) Total apoptotic rate. Results are expressed as mean \pm standard deviation (n=3). *P<0.05 vs. CTRL, **P<0.01 vs. CTRL, #P<0.05 vs. T-2 toxin group. LP-pHS-T2, liposomal delivery system containing T-2 toxin; CTRL, control.

wrapped in the voids of the phospholipid bilayer (48,49). In the present study, the packaging of T-2 toxin was achieved under the condition of a higher drug-to-lipid ratio compared with other reports (25,26). Ultrasound and extrusion steps showed significant effects on the particle size. Following ultrasound, the particle size was distributed in a wide range from 100-500 nm, which was improved after extrusion. Following the optimization of the preparation process, the EE value of LP-pHS-T2 reached $95\pm 2.43\%$. The morphology of LP-pHS-T2 was a spherical shape ~ 100 nm in diameter. LP-pHS-T2 was stable at pH 7.4. The release profile showed a two-phase downward trend starting with a quick release within 10 h, followed by a slow release until reaching a minimum EE value at 72 h. In the measurement of sensitivity to pH of LP-pHS-T2, the remaining T-2 toxin in the sample was immediately detected after incubation for 30 min. It was identified that LP-pHS-T2 released the most toxin at pH 6.5 in the first 30 min of incubation, which indicated that LP-pHS-T2 was extremely sensitive to this pH value, which may be due to the fusogenic properties of lipids. When the pH decreased to 6.5, the carboxyl groups of DPPC and DOPE were sensitively protonated and formed a hexagonal phase structure, which accelerated the drug release by membrane fusion (50). By contrast, at pH values higher or lower than 6.5, only slight amounts of T-2 toxin were released within 30 min. Based on the natural active targeting properties of liposomes, it can be reasonably hypothesized that LP-pHS-T2 may target the pathological tissues, including cancer, inflammation and infection sites, and ischemic areas, in which the pH is known to be lower compared with normal tissue (51).

The antitumor effects of LP-pHS-T2 were tested on a series of tumor cells *in vitro* by MTT assays, with T-2 toxin as the control. The data demonstrated that LP-pHS-T2 can inhibit the proliferation of carcinoma cells. Different types of cells exhibited different degrees of tolerance; K562 cells were most sensitive to T-2 toxin compared with A549, Hep-G2, MKN-45 and L929 cell lines. The difference in IC_{50} values for different cancer cells was due to the toxic mechanism of T-2 toxin. T-2 toxin inhibits cell proliferation by inhibiting some key enzymes involved in protein and nucleic acid synthesis (8). So the greater toxicity of T-2 toxin might be observed in the more vigorously proliferative cells. Furthermore, the IC_{50} value of LP-pHS-T2 on L929 cells was increased by up to 1.3-fold compared with that of T-2 toxin, which indicated

that the side effects of T-2 toxin were decreased. However, although these IC_{50} values were statistically different, as a potential antitumor drug, the safety of LP-pHS-T2 has not been able to meet clinical requirements due to the lack of preclinical studies and its toxicity to normal cells. It remains necessary to modify or further verify its safety through more experiments. Following LP-pHS-T2 and T-2 toxin treatment, apoptosis and cell death occurred, and the migration ability of Hep-G2 cells was significantly inhibited. However, compared to the non-treated group, T-2 toxin and LP-pHS-T2 only caused a slightly increased cell cycle arrest at the G_0/G_1 phase. The mechanism of apoptosis induced by T-2 toxin may be a non-cell cycle dependent pathway (data not shown). Moreover, considering that the pH-sensitive liposomes can be recognized and sequestered by the phagocytes of the reticulo-endothelial system (RES), the clinical use of LP-pHS-T2 remains a future prospect. To avoid their uptake by RES, further reduce the side effects and prolong circulation time, grafting of the liposomal membranes with pegylated phospholipids (52), construction of a programmed nano-selenium overcoat nanoparticles for T-2 toxin (53), or combination of T-2 toxin and multiple targeting carriers may be the solution for LP-pHS-T2 targeted therapy (54).

In summary, the present study investigated LP-pHS-T2, a novel pH-sensitive liposome delivery system containing T-2 toxin; it not only has a release ability in the tumor micro-environment, but also has advantageous antitumor activity *in vitro*. Additionally, due to the encapsulation of liposomes, the side effects of T-2 toxin are relatively reduced. The present study provided a novel approach for the development of T-2 toxin-based anticancer drugs. However, it is important to note that the mechanism and the modification of LP-pHS-T2 on tumor cells require further studies.

Acknowledgements

Not applicable.

Funding

This study was supported by the Program of Administration of Traditional Chinese Medicine of Jilin Province, P.R. China (grant no. 2020132), the Research and Development of Industrial Technology' Program of Jilin Province, P.R. China

(grant nos. 20180623045TC and 20170204005YY), the Program of Jilin Science and Technology Bureau, P.R. China (grant nos. 2019001179 and 20200104093) and the Start Funding of Jilin Medical University (grant no. 2017kyqd001).

Availability of data and materials

The datasets used and/or analyzed during the current study are available from the corresponding author on reasonable request.

Authors' contributions

YD and YL prepared the liposomes. GM performed the HPLC. JG was responsible for cell culture. MY evaluated the pH sensitivity and stability of liposomes. HX analyzed the data regarding the characterization of liposomes. JZ and WZ investigated the antitumor activity of drugs. ML and YL optimized the preparation conditions of liposomes. HW analyzed all the data and wrote the manuscript. All authors read and approved the final manuscript.

Ethics approval and consent to participate

Not applicable.

Patient consent for publication

Not applicable.

Competing interests

The authors declare that they have no competing interests.

References

- Wu J, Zhou Y, Yuan Z, Yi J, Chen J, Wang N and Tian Y: Autophagy and apoptosis interact to modulate T-2 toxin-induced toxicity in liver cells. *Toxins (Basel)* 11: 45, 2019.
- Yang L, Tu D, Wang N, Deng Z, Zhan Y, Liu W, Hu Y, Liu T, Tan L, Li Y, *et al.*: The protective effects of DL-selenomethionine against T-2/HT-2 toxins-induced cytotoxicity and oxidative stress in broiler hepatocytes. *Toxicol In Vitro* 54: 137-146, 2019.
- Meng-Reiterer J, Varga E, Nathanael AV, Bueschl C, Rechthaler J, McCormick SP, Michlmayr H, Malachova A, Fruhmann P, Adam G, *et al.*: Tracing the metabolism of HT-2 toxin and T-2 toxin in barley by isotope-assisted untargeted screening and quantitative LC-HRMS analysis. *Anal Bioanal Chem* 407: 8019-8033, 2015.
- Wang Y, Zhang L, Peng D, Xie S, Chen D, Pan Y, Tao Y and Yuan Z: Construction of electrochemical immunosensor based on gold-nanoparticles/carbon nanotubes/chitosan for sensitive determination of T-2 toxin in feed and swine meat. *Int J Mol Sci* 19: 3895, 2018.
- Seeboth J, Solinhac R, Oswald IP and Guzylack-Piriou L: The fungal T-2 toxin alters the activation of primary macrophages induced by TLR-agonists resulting in a decrease of the inflammatory response in the pig. *Vet Res* 43: 35, 2012.
- Osselaere A, Li SJ, De Bock L, Devreese M, Goossens J, Vandenbroucke V, Van Bocxlaer J, Boussery K, Pasmans F, Martel A, *et al.*: Toxic effects of dietary exposure to T-2 toxin on intestinal and hepatic biotransformation enzymes and drug transporter systems in broiler chickens. *Food Chem Toxicol* 55: 150-155, 2013.
- Doi K, Ishigami N and Sehata S: T-2 toxin-induced toxicity in pregnant mice and rats. *Int J Mol Sci* 9: 2146-2158, 2008.
- Fu YT, Lin WG, BaoCheng Z and Quan G: The effect of T-2 toxin on IL-1 β and IL-6 secretion in human fetal chondrocytes. *Int Orthop* 25: 199-201, 2001.
- Chen X, Xu J, Liu D, Sun Y, Qian G, Xu S, Gan F, Pan C and Huang K: The aggravating effect of selenium deficiency on T-2 toxin-induced damage on primary cardiomyocyte results from a reduction of protective autophagy. *Chem Biol Interact* 300: 27-34, 2019.
- Huang Z, Wang Y, Qiu M, Sun L, Liao J, Wang R, Sun X, Bi S and Gooneratne R: Effect of T-2 toxin-injected shrimp muscle extracts on mouse macrophage cells (RAW264.7). *Drug Chem Toxicol* 41: 16-21, 2018.
- Nathanael AV, Varga E, Meng-Reiterer J, Bueschl C, Michlmayr H, Malachova A, Fruhmann P, Jestoi M, Peltonen K, Adam G, *et al.*: Metabolism of the fusarium mycotoxins T-2 toxin and HT-2 toxin in wheat. *J Agric Food Chem* 63: 7862-7872, 2015.
- Wu Q, Huang L, Liu Z, Yao M, Wang Y, Dai M and Yuan Z: A comparison of hepatic in vitro metabolism of T-2 toxin in rats, pigs, chickens, and carp. *Xenobiotica* 41: 863-873, 2011.
- Konigs M, Mulac D, Scherwdt G, Gekle M and Humpf HU: Metabolism and cytotoxic effects of T-2 toxin and its metabolites on human cells in primary culture. *Toxicology* 258: 106-115, 2009.
- Wang J, Yang C, Yuan Z, Yi J and Wu J: T-2 toxin exposure induces apoptosis in TM3 cells by inhibiting mammalian target of rapamycin/serine/threonine protein kinase(mTORC2/AKT) to promote Ca²⁺ production. *Int J Mol Sci* 19: 3360, 2018.
- Ueno Y, Umemori K, Niimi E, Tanuma S, Nagata S, Sugamata M, Ihara T, Sekijima M, Kawai K, Ueno I, *et al.*: Induction of apoptosis by T-2 toxin and other natural toxins in HL-60 human promyelotic leukemia cells. *Nat Toxins* 3: 129-137, 1995.
- Nagase M, Alam MM, Tsushima A, Yoshizawa T and Sakato N: Apoptosis induction by T-2 toxin: Activation of caspase-9, caspase-3, and DFF-40/CAD through cytosolic release of cytochrome c in HL-60 cells. *Biosci Biotechnol Biochem* 65: 1741-1747, 2001.
- Chaudhari M, Jayaraj R, Bhaskar AS and Lakshmana Rao PV: Oxidative stress induction by T-2 toxin causes DNA damage and triggers apoptosis via caspase pathway in human cervical cancer cells. *Toxicology* 262: 153-161, 2009.
- Gao C, Zhang Y, Chen J, Wang T, Qian Y, Yang B, Dong P and Zhang Y: Targeted drug delivery system for platinum-based anticancer drugs. *Mini Rev Med Chem* 16: 872-891, 2016.
- T S A, Shalumon KT and Chen JP: Applications of magnetic liposomes in cancer therapies. *Curr Pharm Des* 25: 1490-1504, 2019.
- Paliwal SR, Paliwal R and Vyas SP: A review of mechanistic insight and application of pH-sensitive liposomes in drug delivery. *Drug Deliv* 22: 231-242, 2015.
- Shaban N, Abdel-Rahman S, Haggag A, Awad D, Bassiouny A and Talaat I: Combination between taxol-encapsulated liposomes and eruca sativa seed extract suppresses mammary tumors in female rats induced by 7,12 dimethylbenz(α)anthracene. *Asian Pac J Cancer Prev* 17: 117-123, 2016.
- Cadinoiu AN, Rata DM, Atanase LI, Daraba OM, Gherghel D, Vochita G and Popa M: Aptamer-functionalized liposomes as a potential treatment for basal cell carcinoma. *Polymers (Basel)* 11: 1515, 2019.
- Yang Y, Yang X, Li H, Li C, Ding H, Zhang M, Guo Y and Sun M: Near-infrared light triggered liposomes combining photodynamic and chemotherapy for synergistic breast tumor therapy. *Colloids Surf B Biointerfaces* 173: 564-570, 2019.
- Sadeghi N, Kok RJ, Bos C, Zandvliet M, Geerts WJC, Storm G, Moonen CTW, Lammers T and Deckers R: Hyperthermia-triggered release of hypoxic cell radiosensitizers from temperature-sensitive liposomes improves radiotherapy efficacy in vitro. *Nanotechnology* 30: 264001, 2019.
- Odette WL, Payne NA, Khaliullin RZ and Mauzeroll J: Redox-triggered disassembly of nanosized liposomes containing ferrocene-appended amphiphiles. *Langmuir* 35: 5608-5616, 2019.
- Li B, Li B, He D, Feng C, Luo Z and He M: Preparation, characterization, and in vitro pH-sensitivity evaluation of superparamagnetic iron oxide nanoparticle- misonidazole pH-sensitive liposomes. *Curr Drug Deliv* 16: 254-267, 2019.
- Chen Y, Du Q, Guo Q, Huang J, Liu L, Shen X and Peng J: A W/O emulsion mediated film dispersion method for curcumin encapsulated pH-sensitive liposomes in the colon tumor treatment. *Drug Dev Ind Pharm* 45: 282-291, 2019.
- Duan Y, Wei L, Petryk J and Ruddy TD: Formulation, characterization and tissue distribution of a novel pH-sensitive long-circulating liposome-based theranostic suitable for molecular imaging and drug delivery. *Int J Nanomedicine* 11: 5697-5708, 2016.

29. Chiang NJ, Chao TY, Hsieh RK, Wang CH, Wang YW, Yeh CG and Chen LT: A phase I dose-escalation study of PEP02 (irinotecan liposome injection) in combination with 5-fluorouracil and leucovorin in advanced solid tumors. *BMC Cancer* 16: 907, 2016.
30. Rehman AU, Omran Z, Anton H, Mely Y, Akram S, Vandamme TF and Anton N: Development of doxorubicin hydrochloride loaded pH-sensitive liposomes: Investigation on the impact of chemical nature of lipids and liposome composition on pH-sensitivity. *Eur J Pharm Biopharm* 133: 331-338, 2018.
31. Riondel J, Jacrot M, Fessi H, Puisieux F and Potier: Effects of free and liposome-encapsulated taxol on two brain tumors xenografted into nude mice. *In Vivo* 6: 23-27, 1992.
32. Rubio DP, Roa LG, Soto DA, Velasquez FJ, Gregorcic NA, Soto JA, Martinez MC, Kalergis AM and Vasquez AE: Purification and characterization of saxitoxin from *mytilus chilensis* of southern Chile. *Toxicon* 108: 147-153, 2015.
33. Shi R, Xu X, Wu J, Wang T, Li Y, Ma B and Ma Y: Hydrophilic interaction chromatography-tandem mass spectrometry based on an amide column for the high-throughput quantification of metformin in rat plasma. *RSC Adv* 5: 101386-101392, 2015.
34. Zhang H: Thin-film hydration followed by extrusion method for liposome preparation. *Methods Mol Biol* 1522: 17-22, 2017.
35. Liu GX, Fang GQ and Xu W: Dual targeting biomimetic liposomes for paclitaxel/DNA combination cancer treatment. *Int J Mol Sci* 15: 15287-15303, 2014.
36. Dornetshuber-Fleiss R, Heilos D, Mohr T, Richter L, Sussmuth RD, Zlesak M, Novicky A, Heffeter P, Lemmens-Gruber R and Berger W: The naturally born fusariotoxin enniatin B and sorafenib exert synergistic activity against cervical cancer in vitro and in vivo. *Biochem Pharmacol* 93: 318-331, 2015.
37. Song J, Wang Y, Teng M, Zhang S, Yin M, Lu J, Liu Y, Lee RJ, Wang D and Teng L: *Cordyceps militaris* induces tumor cell death via the caspase-dependent mitochondrial pathway in HepG2 and MCF-7 cells. *Mol Med Rep* 13: 5132-5140, 2016.
38. Ovejero S, Ayala P, Malumbres M, Pimentel-Muinos FX, Bueno A and Sacristan MP: Biochemical analyses reveal amino acid residues critical for cell cycle-dependent phosphorylation of human Cdc14A phosphatase by cyclin-dependent kinase 1. *Sci Rep* 8: 11871, 2018.
39. Belwal VK and Singh KP: Nanosilica-supported liposome (protocells) as a drug vehicle for cancer therapy. *Int J Nanomedicine* 13: 125-127, 2018.
40. Soema PC, Willems GJ, Jiskoot W, Amorij JP and Kersten GF: Predicting the influence of liposomal lipid composition on liposome size, zeta potential and liposome-induced dendritic cell maturation using a design of experiments approach. *Eur J Pharm Biopharm* 94: 427-435, 2015.
41. Zhang X, Wang Y, Velkov T, Tang S and Dai C: T-2 toxin-induced toxicity in neuroblastoma-2a cells involves the generation of reactive oxygen, mitochondrial dysfunction and inhibition of Nrf2/HO-1 pathway. *Food Chem Toxicol* 114: 88-97, 2018.
42. Yu FF, Lin XL, Yang L, Liu H, Wang X, Fang H, Lammi ZJ and Guo X: Comparison of T-2 toxin and HT-2 toxin distributed in the skeletal system with that in other tissues of rats by acute toxicity test. *Biomed Environ Sci* 30: 851-854, 2017.
43. Kojima S, Nakamura N, Ueno Y, Yamaguchi T and Takahashi T: Anti-tumor activity of T-2 toxin-conjugated A7 monoclonal antibody (T-2-A7 MoAb) against human colon carcinoma. *Nat Toxins* 1: 209-215, 1993.
44. Ferreira Ddos S, Lopes SC, Franco MS and Oliveira MC: pH-sensitive liposomes for drug delivery in cancer treatment. *Ther Deliv* 4: 1099-1123, 2013.
45. Bellat V, Lee HH, Vahdat L and Law B: Smart nanotransformers with unique enzyme-inducible structural changes and drug release properties. *Biomacromolecules* 17: 2040-2049, 2016.
46. Yi XQ, Zhang Q, Zhao D, Xu JQ, Zhong ZL, Zhuo RX and Li F: Preparation of pH and redox dual-sensitive core crosslinked micelles for overcoming drug resistance of DOX. *Polym Chem* 7: 1719-1729, 2016.
47. Ruttala HB, Ramasamy T, Gupta B, Choi HG, Yong CS and Kim JO: Multiple polysaccharide-drug complex-loaded liposomes: A unique strategy in drug loading and cancer targeting. *Carbohydr Polym* 173: 57-66, 2017.
48. Vlassov A, Khvorova A and Yarus M: Binding and disruption of phospholipid bilayers by supramolecular RNA complexes. *Proc Natl Acad Sci USA* 98: 7706-7711, 2001.
49. Falck E, Patra M, Karttunen M, Hyvonen MT and Vattulainen I: Impact of cholesterol on voids in phospholipid membranes. *J Chem Phys* 121: 12676-12689, 2004.
50. Bellavance MA, Poirier MB and Fortin D: Uptake and intracellular release kinetics of liposome formulations in glioma cells. *Int J Pharm* 395: 251-259, 2010.
51. Drummond DC, Zignani M and Leroux J: Current status of pH-sensitive liposomes in drug delivery. *Prog Lipid Res* 39: 409-460, 2000.
52. Ramasamy T, Haidar ZS, Tran TH, Choi JY, Jeong JH, Shin BS, Choi HG, Yong CS and Kim JO: Layer-by-layer assembly of liposomal nanoparticles with PEGylated polyelectrolytes enhances systemic delivery of multiple anticancer drugs. *Acta Biomater* 10: 5116-5127, 2014.
53. Ramasamy T, Ruttala HB, Sundaramoorthy P, Poudel BK, Youn YS, Ku SK, Choi HG, Yong CS and Kim JO: Multimodal selenium nanoshell-capped Au@mSiO₂ nanoplatform for NIR-responsive chemo-photothermal therapy against metastatic breast cancer. *NPG Asia Mater* 10: 197-216, 2018.
54. Ramasamy T, Ruttala HB, Kaliraj K, Poudel K, Jin SG, Choi HG, Ku SK, Yong CS and Kim JO: Polypeptide derivative of metformin with the combined advantage of a gene carrier and anticancer activity. *ACS Biomater Sci Eng* 5: 5159-5168, 2019.